# Detailed modeling of dust distribution in the disk of HD 142527
Kang-Lou Soon+ Accepted PASJ

We investigate the dust distribution in the crescent disk around HD 142527 based on the continuum emission at 890 μm obtained by ALMA Cycle 0. The map is divided into 18 azimuthal sectors, and the radial intensity profile in each sector is reproduced with a 2D disk model. Our model takes account of scattering and inclination of the disk as well as the azimuthal dependence in intensity. When the dust is assumed to have the conventional composition and maximum size of 1 mm, the northwestern region ($PA = 329° - 29°$) cannot be reproduced. This is because the model intensity gets insensitive to the increase in surface density due to heavy self-scattering, reaching its ceiling much lower than the observed intensity. The ceiling depends on the position angle. When the scattering opacity is reduced by a factor of 10, the intensity distribution is reproduced successfully in all the sectors including those in the northwestern region. The best fit model parameters depend little on the scattering opacity in the southern region where the disk is optically thin. The contrast of dust surface density along PA is derived to be about 40, much smaller than the value for the cases of conventional opacities ($70 - 130$). These results strongly suggest that the albedo is lower than considered by some reasons at least in the northwestern region.

$$\log\left[I^*_{obs} / \left(1\ \mathrm{Jy\ asec}^{-2}\right)\right]$$

ALMA λ=890μm

major axis
$PA' = 0°$

far side

near side
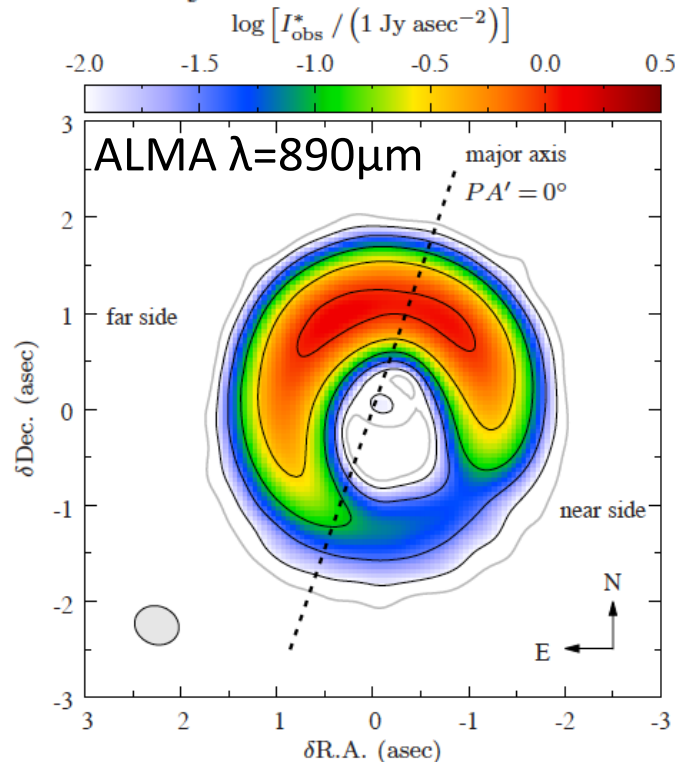
HD142527 中質量前主系列星
ALMA Cycle0
18個のセクターごとにガウス関数でフィット

$$I^*_{obs}(r^*_{obs}) = I^*_{0,obs}\ \exp\left[-\left(\frac{r^*_{obs} - r^*_{0,obs}}{w^*_{0,obs}}\right)^2\right],$$

1 $\Sigma(r) = \Sigma_0\ \exp\left\{-\min\left[\left(\frac{r - r_0}{w_0}\right)^2, 20\right]\right\},$

2   ρ(r,z), T(r,z), J(r,z) LTE + hydrostatic balance

3   Calculate I

通常期待されるダストamax=1mm ではPA=329~29合わない。
散乱不透明度を1/10にするとすべてのセクターで一致。

Redistribution of CO at the Location of the CO Ice Line in evolving Gas and Dust Disks
S. M. Stammler+ AAp Accepted

Context. Ice lines are suggested to play a significant role in grain growth and planetesimal formation in protoplanetary disks. Evaporation fronts directly influence the gas and ice abundances of volatile species in the disk and therefore the coagulation physics and efficiency and the chemical composition of the resulting planetesimals.

Aims. In this work, we investigate the influence of the existence of the CO ice line on particle growth and on the distribution of CO in the disk.

Methods. We include the possibility of tracking the CO content and/or other volatiles in particles and in the gas in our existing dust coagulation and disk evolution model and present a method for studying evaporation and condensation of CO using the Hertz-Knudsen equation. Our model does not yet include fragmentation, which will be part of further investigations.

Results. We find no enhanced grain growth immediately outside the ice line where the particle size is limited by radial drift. Instead, we find a depletion of solid material inside the ice line, which is solely due to evaporation of the CO. Such a depression inside the ice line may be observable and may help to quantify the processes described in this work. Furthermore, we find that the viscosity and diffusivity of the gas heavily influence the re-distribution of vaporized CO at the ice line and can lead to an increase in the CO abundance by up to a factor of a few in the region just inside the ice line. Depending on the strength of the gaseous transport mechanisms, the position of the ice line in our model can change by up to ~ 10 AU and consequently, the temperature at that location can range from 21 to 23 K.

1.gas
$$\frac{\partial}{\partial t}\Sigma_j + \frac{1}{R}\frac{\partial}{\partial R}\left(R\Sigma_j u_{gas}\right) - \frac{3}{R}\frac{\partial}{\partial R}\left[R\Sigma_{gas}\nu\frac{\partial}{\partial R}\left(\frac{\Sigma_j}{\Sigma_{gas}}\right)\right] = 0. \qquad (6)$$

inflow   α-viscosity

the Schmidt number Sc = ν/D; which is the ratio of viscosity ν to diffusivity D of a gas

2.dust
$$\frac{\partial}{\partial t}\Sigma_{dust,i} + \frac{1}{R}\frac{\partial}{\partial R}\left(R\left[\Sigma_{dust,i}u_{dust,i} - D_{dust,i}\Sigma_{gas}\frac{\partial}{\partial R}\frac{\Sigma_{dust,i}}{\Sigma_{gas}}\right]\right) = 0,$$

bulk inflow   particle 拡散   (15)

$$u_{dust,i} = \frac{u_{gas}}{1 + St_i^2} - \frac{2u_P}{St_i + St_i^{-1}}. \qquad (16)$$

gas drag   head wind

$$St = \frac{\tau_s}{\tau_{ed}}.$$
stopping time
eddy turn over time

Epstein則 $\tau_s = \frac{\rho_s a}{\rho_{gas}\bar{u}}$,
ダスト物質密度
サイズ
ガス分子熱速度

$$u_P = -\frac{\frac{\partial}{\partial R}P_{gas}}{2\rho_{gas}\Omega_K}.$$

3.dust coaguration
$$\frac{\partial}{\partial t}f(m) = \frac{1}{2}\int_0^\infty dm'\int_0^\infty dm'' f(m') f(m'') K(m';m'') \times$$
$$\times \delta(m' + m'' - m)$$

Smoluchowski eq. $-f(m)\int_0^\infty dm' f(m') K(m;m'),$ (19)

4.evaporation+condensation
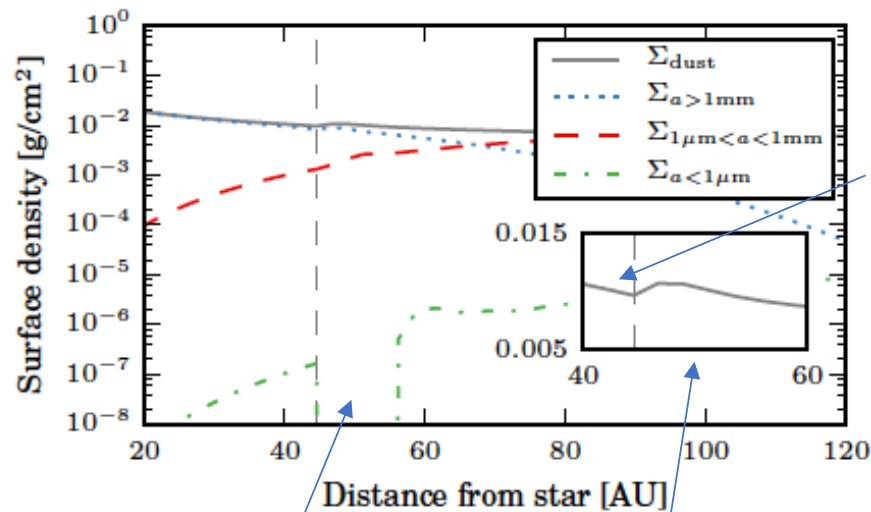
ice-line 外側でダストの成長

すぐ内側で減る
CO蒸発

Fig. 2. Dust surface densities of different dust sizes at the CO ice line after 1 Myr. Shown are the total surface density (solid gray line), millimeter-sized (dotted blue line), sub-millimeter-sized (*dashed red line*), and sub-micrometer-sized (dash-dotted green line) particles. The vertical dashed line marks the location of the CO ice line.

CO気体のice-line内側からの拡散
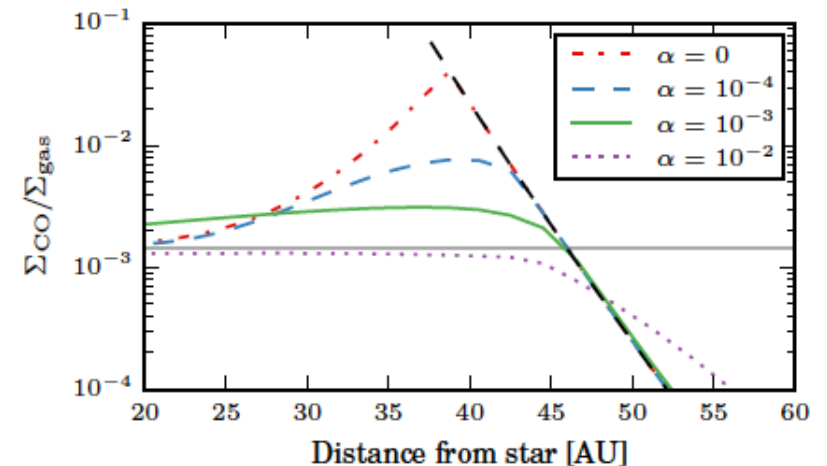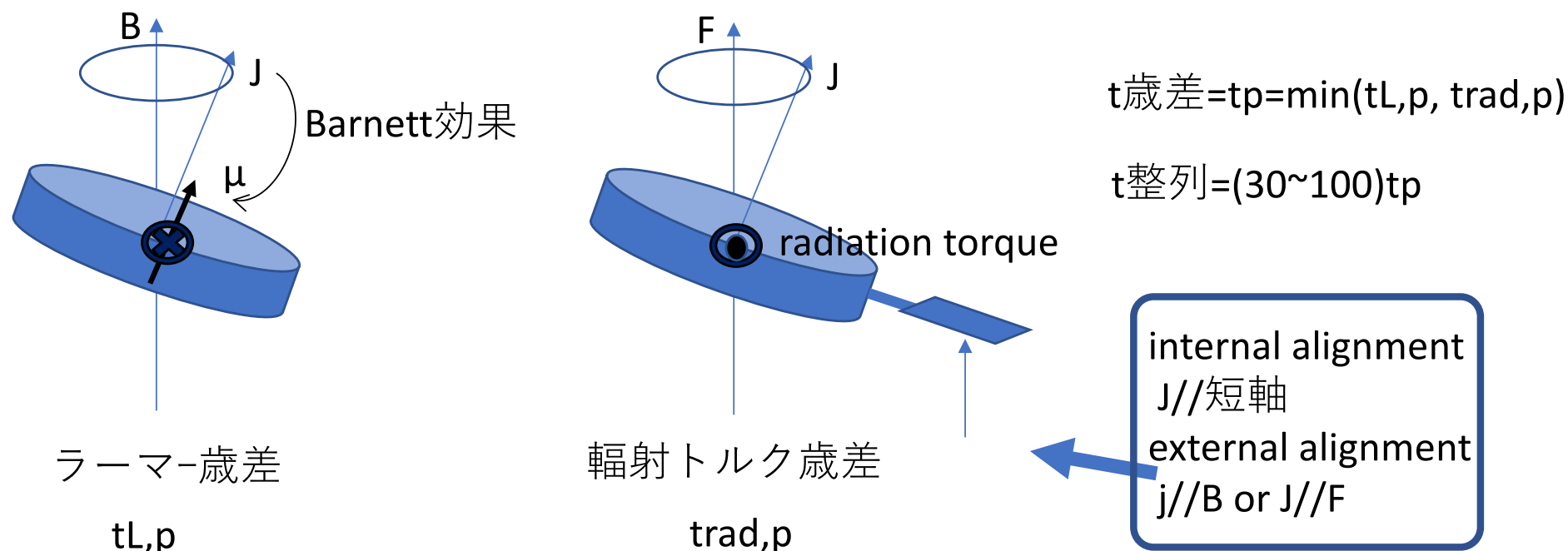ダスト全量に効くほどではない

粘性、拡散係数COガス割合分布に
効く

Fig. 7. The ratio of CO gas surface density to total gas surface density after 1 Myr in the region of the ice line. Shown are the fiducial model with $\alpha = 10^{-3}$ (solid green line), a low-viscosity model with $\alpha = 10^{-4}$ (dashed blue), and a high-viscosity model with $\alpha = 10^{-2}$ (dotted purple). The ratio of $\Sigma_{CO}^{eq}/\Sigma_{gas}$ is plotted with a dashed black line. Also plotted is the case of a disk without viscous spreading (red dash-dotted line). The horizontal gray line is our input value for the CO-to-gas mass ratio.
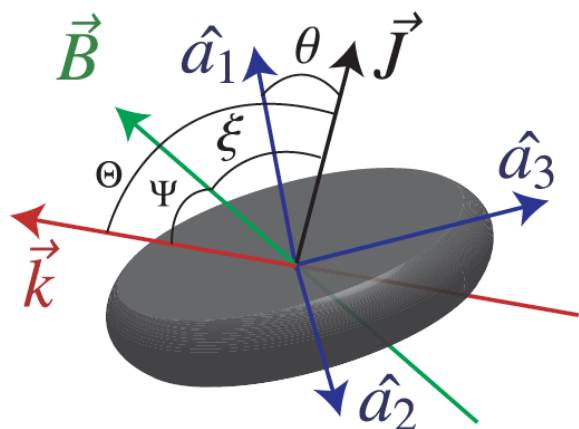
Radiative grain alignment in protoplanetary disks: Implications for polarimetric observations
Ryo Tazaki[1,2], Alexandre Lazarian [3], and Hideko Nomura ApJ in press

We apply the theory of radiative torque (RAT) alignment for studying protoplanetary disks around a T-Tauri star and perform 3D radiative transfer calculations to provide the expected maps of polarized radiation to be compared with observations, such as with ALMA. We revisit the issue of grain alignment for large grains expected in the protoplanetary disks and find that mm-sized grains at midplane do not align with magnetic field as the Larmor precession timescale for such large grains becomes longer than the gaseous damping timescale. Hence, for these grains the RAT theory predicts that the alignment axis is determined by the grain precession with respect to the radiative flux. As a result, we expect that the polarization will be in the azimuthal direction for a face-on disk. It is also shown that if dust grains have superparamagnetic inclusions, magnetic field alignment is possible for (sub-)micron grains at the surface layer of disks, and this can be tested by mid-infrared polarimetric observations.

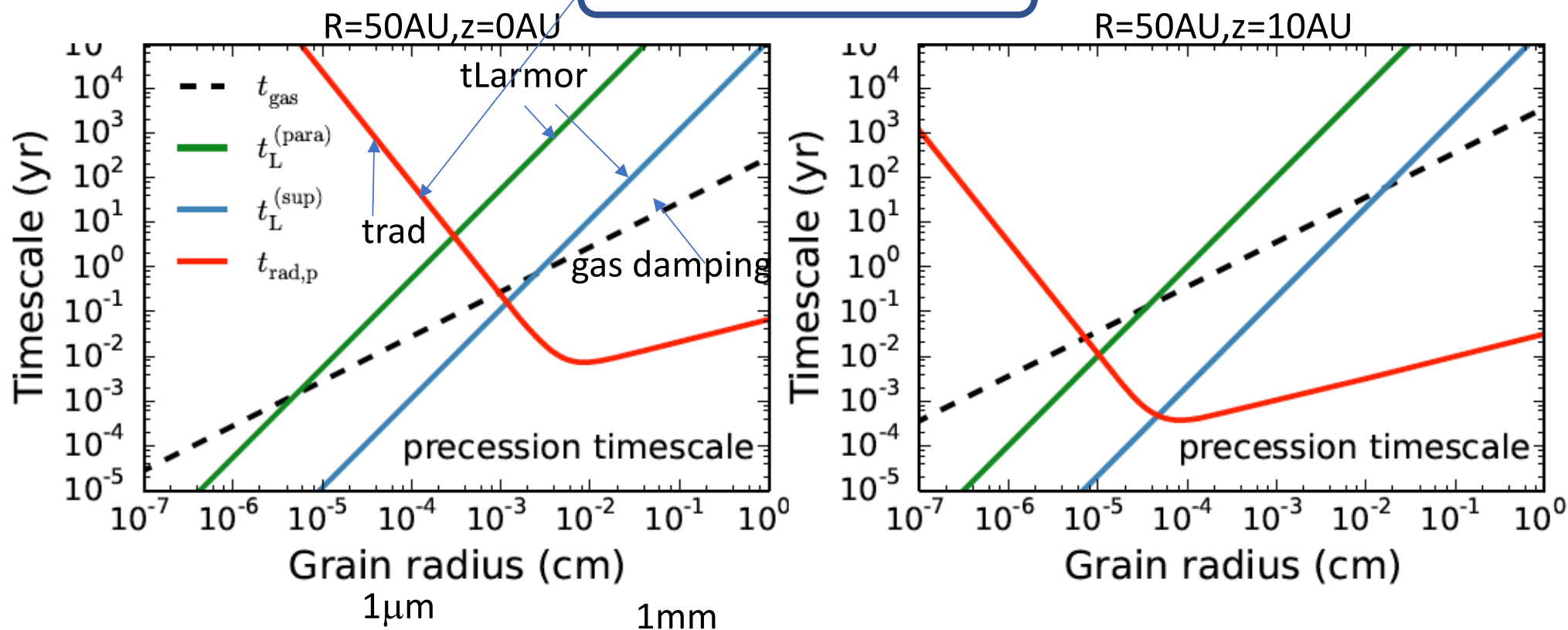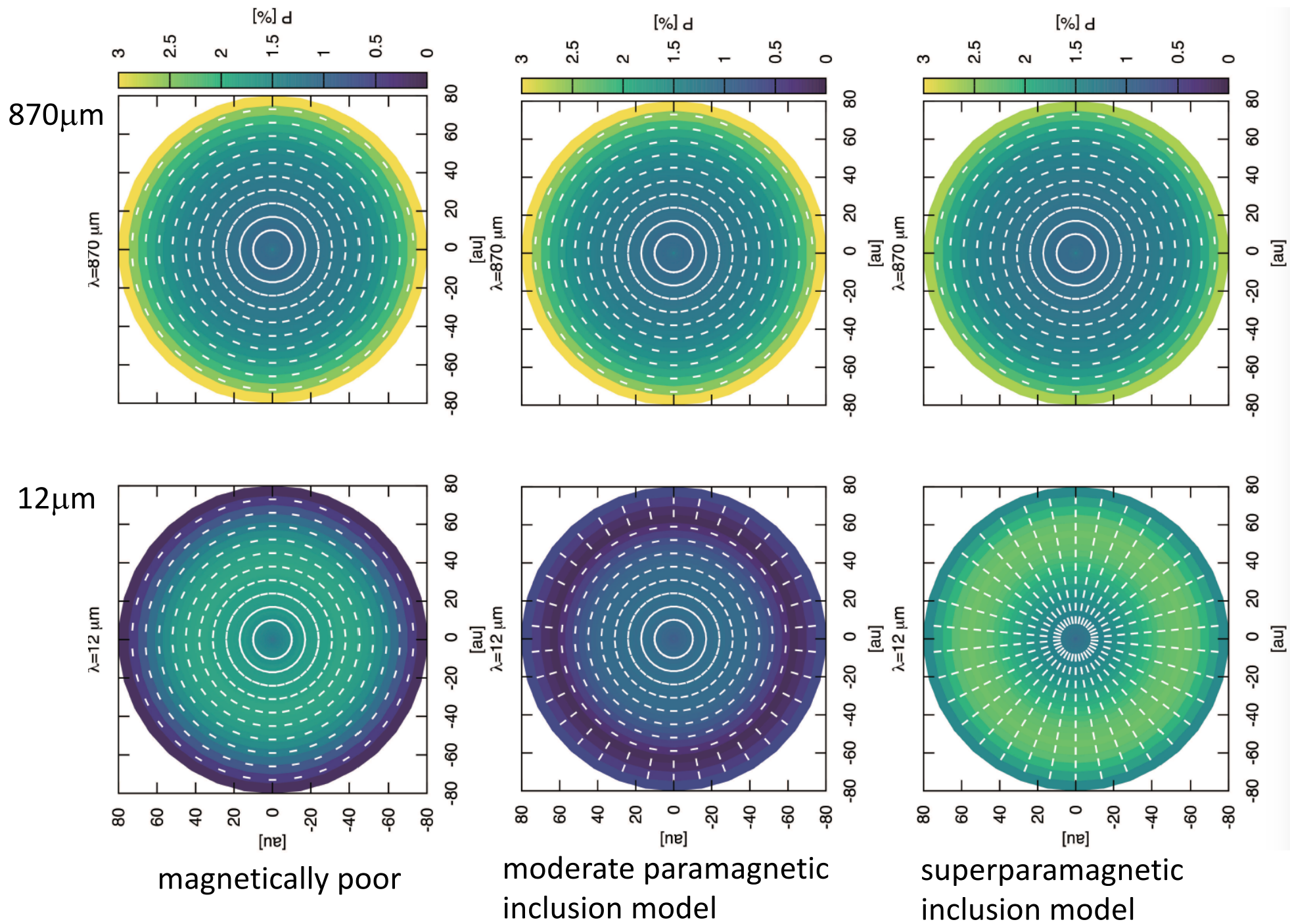*Keywords:* dust, extinction — polarization — protoplanetary disks — radiative transfer

B

J

Barnett効果

μ

ラーマー歳差

tL,p

F

J

radiation torque

輻射トルク歳差

trad,p

t歳差=tp=min(tL,p, trad,p)

t整列=(30~100)tp

internal alignment
J//短軸
external alignment
j//B or J//F

rad. torque 効率

$$|Q_\Gamma| \approx 2.3 \left(\frac{\lambda}{a_{\text{eff}}} \right)^{-3} \quad \text{for } \lambda > 1.8 a_{\text{eff}}$$

$$\approx 0.4 \qquad \text{for } \lambda \leq 1.8 a_{\text{eff}}$$

R=50AU,z=0AU

tLarmor

- - - t_{gas}
— $t_{\text{L}}^{(\text{para})}$
— $t_{\text{L}}^{(\text{sup})}$
— $t_{\text{rad,p}}$

trad

gas damping

precession timescale

1μm   1mm

R=50AU,z=10AU

precession timescale

870μm

12μm

magnetically poor

moderate paramagnetic
inclusion model

superparamagnetic
inclusion model

54. Accretion and Magnetic Reconnection in the Classical T Tauri Binary DQ Tau
Benjamin Tofflemire+ Accepted by ApJ

The theory of binary star formation predicts that close binaries ($a < 100$ au) will experience periodic pulsed accretion events as streams of material form at the inner edge of a circumbinary disk (CBD), cross a dynamically cleared gap, and feed circumstellar disks or accrete directly onto the stars. The archetype for the pulsed accretion theory is the eccentric, short-period, classical T Tauri binary DQ Tau. Low-cadence (~daily) broadband photometry has shown brightening events near most periastron passages, just as numerical simulations would predict for an eccentric binary. Magnetic reconnection events (flares) during the collision of stellar magnetospheres near periastron could, however, produce the same periodic, broadband behavior when observed at a one-day cadence. To reveal the dominant physical mechanism seen in DQ Tau's low-cadence observations, we have obtained continuous, moderate-cadence, multiband photometry over 10 orbital periods, supplemented with 27 nights of minute-cadence photometry centered on four separate periastron passages. While both accretion and stellar flares are present, the dominant timescale and morphology of brightening events are characteristic of accretion. On average, the mass accretion rate increases by a factor of five near periastron, in good agreement with recent models. Large variability is observed in the morphology and amplitude of accretion events from orbit to orbit. We argue that this is due to the absence of stable circumstellar disks around each star, compounded by inhomogeneities at the inner edge of the CBD and within the accretion streams themselves. Quasiperiodic apastron accretion events are also observed, which are not predicted by binary accretion theory.

周期的に生じるaccretion stream
鋭さは離心率による

gap

circumstellar disk

circumbinary disk

circular orbit
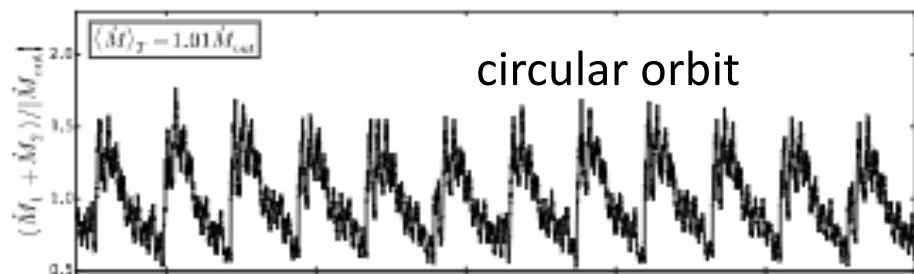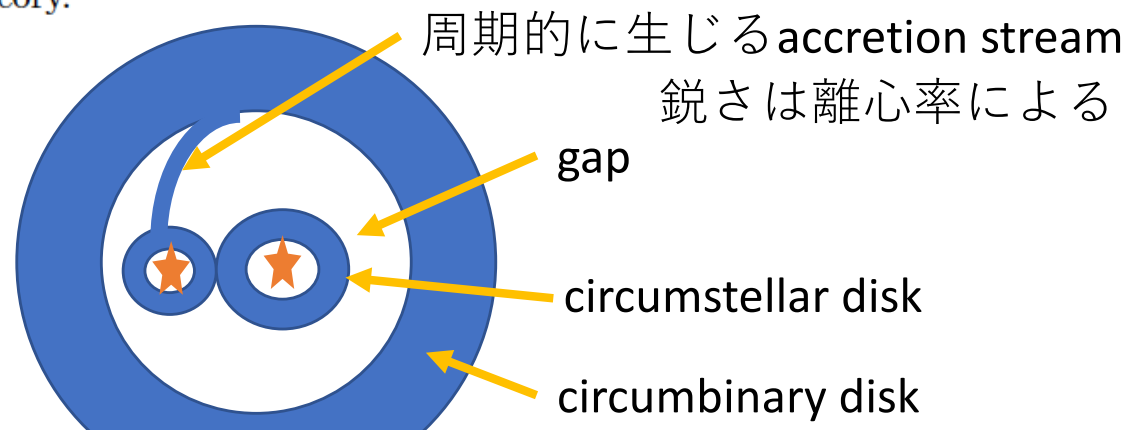
Muñoz + Lai 2016
1. the moving-mesh code AREPO
2. circumbinary accretion onto eccentric and circular binaries
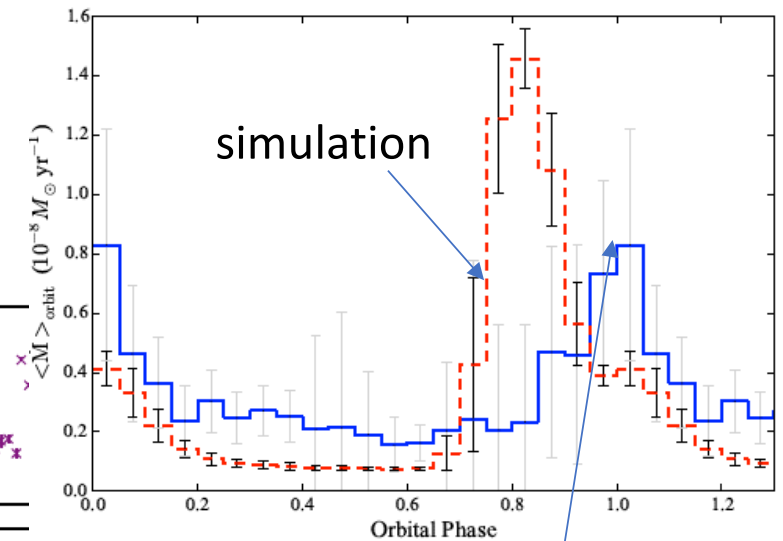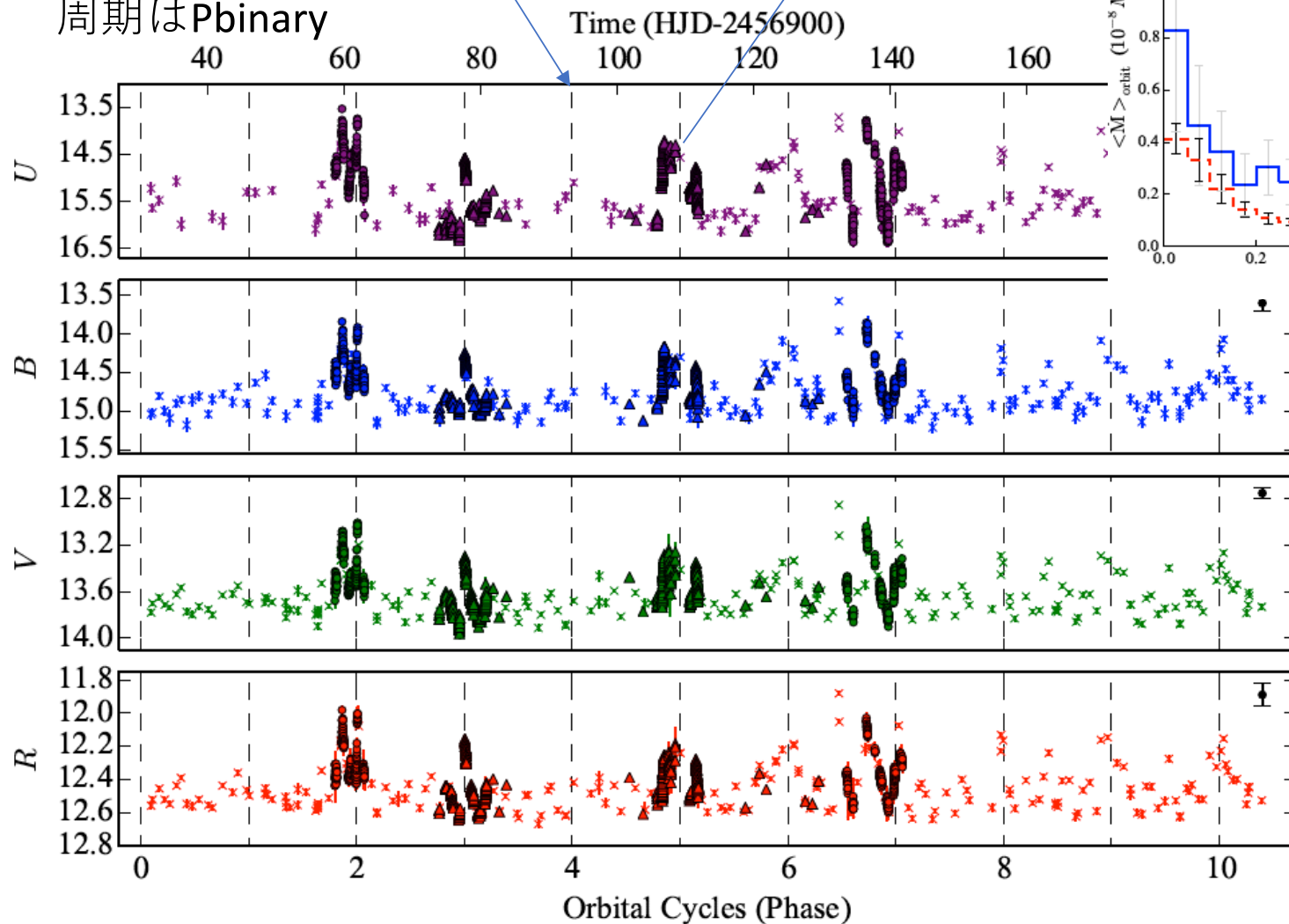3. circular:period~5Pbinary
　　eccentric : ~ 1Pbinary, 各星の Mdotは10~20倍異なる

eccentric orbit　　　10Pb

t
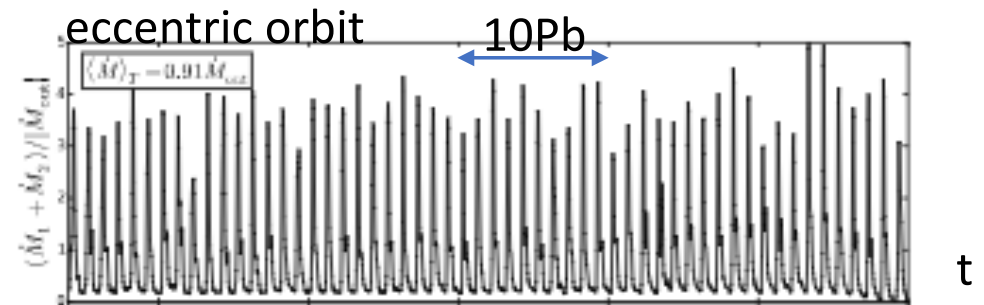
DQ Tau pre-MS spectroscopic binary

P (days)	15.80158 ± 0.00066
e	0.568 ± 0.013
T_{peri} (HJD-2,400,000)	47433.507 ± 0.094
a ($R_\odot$)	28.96 ± 0.48
q ≡ M2/M1	0.936 ± 0.051

$$\dot{M} \simeq \frac{L_{\mathrm{Acc}} R_\star}{G M_\star} \left(1 - \frac{R_\star}{R_{\mathrm{in}}}\right)^{-1}, \qquad (2)$$

periastron 近辺で増光する

周期はPbinary

simulation

Mdot~5倍くらい増

55. Grand-design Spiral Arms in a Young Forming Circumstellar Disk

K. Tomida, M. N. Machida, T. Hosokawa, Y. Sakurai and C. H. Lin; Accepted by ApJL

We study formation and long-term evolution of a circumstellar disk in a collapsing molecular cloud core using a resistive magnetohydrodynamic simulation. While the formed circumstellar disk is initially small, it grows as accretion continues, and its radius becomes as large as 200 au toward the end of the Class-I phase. A pair of grand-design spiral arms form due to gravitational instability in the disk, and they transfer angular momentum in the highly resistive disk. Although the spiral arms disappear in a few rotations as expected in a classical theory, new spiral arms form recurrently as the disk soon becomes unstable again by gas accretion. Such recurrent spiral arms persist throughout the Class-0 and I phases. We then perform synthetic observations and compare our model with a recent high-resolution observation of a young stellar object Elias 227, whose circumstellar disk has grand-design spiral arms. We find good agreement between our theoretical model and the observation. Our model suggests that the grand-design spiral arms around Elias 227 are consistent with material arms formed by gravitational instability. If such spiral arms commonly exist in young circumstellar disks, it implies that young circumstellar disks are considerably massive and gravitational instability is the key process of angular momentum transport.
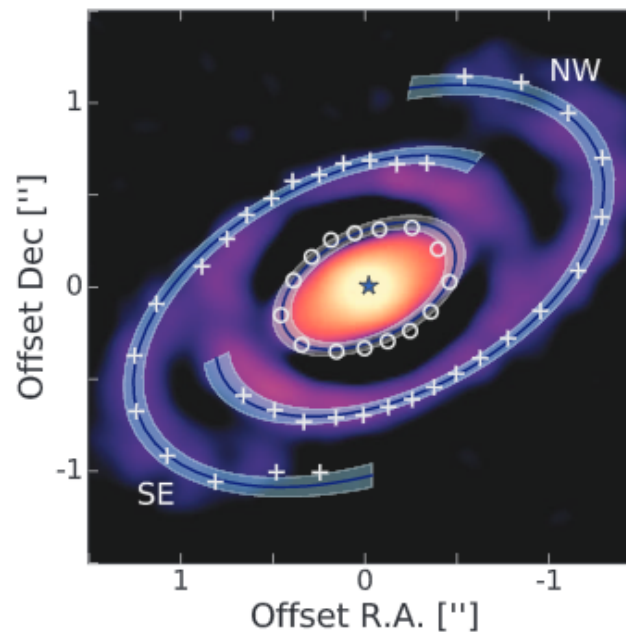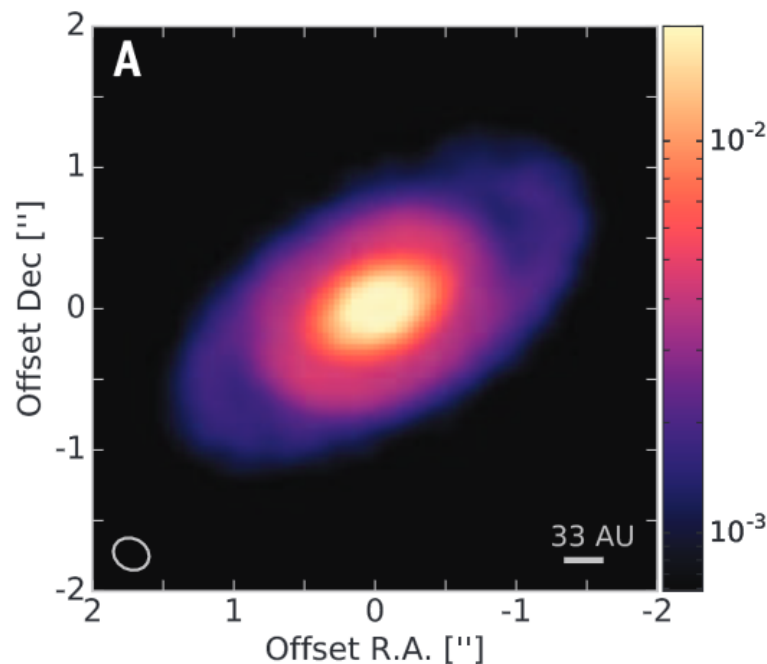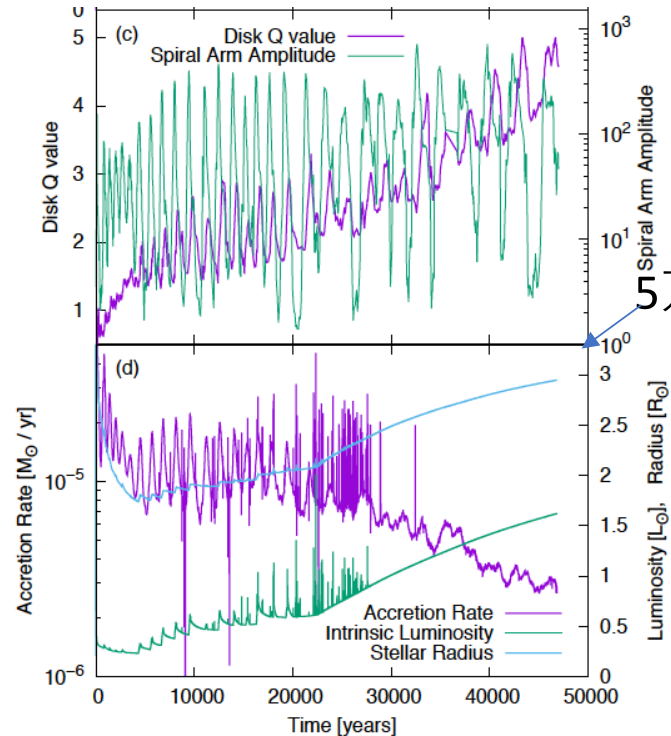
Elias 2-27
Pérez + 2016 Science
"We argue that the observed spirals trace shocks of spiral density waves in the midplane of this young disk."

resistive MHD + nested grid + barotropic + Ohmic dissipation + 中心 sink cell

episodic accretion by self-grav. insta.   中心星の光の輸送 RADMC-3D

5万年